Publishing House
AKAPIT

COMPUTER METHODS IN MATERIALS SCIENCE

Informatyka w Technologii Materiałów

Vol. 6, 2006, No. 3-4

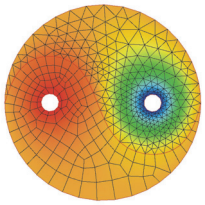

NUMERICAL SIMULATION OF ELASTOPLASTIC DEFORMATION OF THIN HARD COATING SYSTEMS IN NANO-IMPACT TEST

MAGDALENA KOPERNIK, MACIEJ PIETRZYK, ANDRZEJ ŻMUDZKI

Department of Modelling and Information Technology, Akademia Górniczo-Hutnicza
Mickiewicza 30, 30-059 Kraków, Poland; pietrzyk@metal.agh.edu.pl

Abstract

Development of the finite element model of nano-impact tests is the objective of the paper. Although these tests are performed to determine, among others, the crack resistance of nanocoatings, there is no fracture criterion introduced in the model at this stage. Research is focused on overcoming various difficulties occurring in finite element simulation of deformation of thin hard coating systems. These difficulties arise from layers thickness, necessity of remeshing, multi-material and multi-impact character of simulation, which has to connect different types of numerical solutions simultaneously. The simulations were performed using Forge 2 code adapted to the thin layer conditions. Problems with adaptation and scaling are described. Selected results of simulations are presented in the paper. Since it is capable to predict realistic stress and strain fields, the developed model is prepared to implementation of the fracture criterion.

Key words: hard coating system, FEM, nano-impact test, plastic deformation, FGM

1. INTRODUCTION

Thin multilayers are manufactured as functionally graded materials (FGM) and they have characteristic features. FGMs have innovative properties and/or functions that cannot be achieved by conventional homogeneous materials (Dao et al., 1997; Kopernik and Pietrzyk, 2006). Due to very small scale and very contrasting physical properties in adjacent layers, graded nano materials are challenging in experiments and in simulations (Beake and Smith, 2004; Paszyński et al., 2006). Finite element method (FEM) (Zienkiewicz and Taylor, 2000) helps to solve designing problems, to control various processes and to anticipate materials behaviour (Kopernik and Pietrzyk, 2006).

In order to determine their properties, thin films and coatings are deformed in nanoindentation tests under low, constant in time loads. Elastic or elasto-plastic deformations are involved depending on the material. Velocity of moving tool in low load, static test should not generate a fracture. Since it is not an aim of the nanoindentation test, there is no fracture examination of specimens. This experiment gives rather information about material hardness, which is calculated on the basis of load measurements. Small cracks connected with the test conditions, especially interaction between really very hard coating and diamond indenter, may occur only in the die/specimen contact region, but they should be definitely avoided.

Contrary, the objective of nano-impact tests is evaluation of material crack resistance and these tests involve cracks. The material fracture during impact test is caused by an acceleration of the moving tool. The tool hits surface of the specimen and produces effect similar to shock waves, which propagate in a material. These waves cause high

 ISSN 1641-8581

values of stress and strain, which are observed in elastoplastic coatings (plastic part of material model is responsible for fracture occurrence). Elastic coatings transmit loadings and do not accumulate strain. Similarly to nanoindentation, the nano-impact technique is also a low load test, but not a static one. The total value of mechanical energy (load energy – nJ, μJ) is the same in both tests, but the method and the purpose of its use is different. Working conditions of nano layers are reproduced in the impact test and it helps to determine time and location of fracture under different exploitation conditions. In consequence, this test is capable of revealing marked differences in performance that can be used to optimise the design of coating systems for improved durability. Instead of simply characterizing coatings and thin films, their actual tribological performance under "in-service" conditions can now be assessed.

Due to very small scale of the experiment and several disturbances, direct interpretation of the results of nano-impact tests is difficult. On the other hand, numerical models can simulate thin films behaviour in the experiment and reveal the real state of strains and stresses. Thus, the finite element (FEM) simulation of the nano-impact test is the main objective of the present work The experience gained in modelling of nanoindentation test, which gave results comparable to experimental ones (Kopernik and Pietrzyk, 2007), is used in this work.

The particular objective of the present project is analysis of stress and strain states in the nano-impact test and fracture criterion is not introduced at this stage. The developed model will be further extended by implementation of fracture criteria in the future. These criteria are defined as relations with stress and strains, therefore, information supplied by the present model will be an input to those criteria. Developed model will be also combined with the optimization techniques and used in the inverse analysis of the low load nanotests.

2. MATERIALS

2.1. Specimen description

Thin hard coating systems are investigated in this article and they are commented upon meaning of designing ability, which is achieved in predicting material behaviour and properties in nano-impact test. The main designing rules used in producing these systems come from tribology and are set into material in manufacturing process. Such rules are visible in products, which are analysed in the paper, because they are tribological coatings of third generation.

The idea of multilayer system manufacturing arises from tribological observations coupling elastic and elastoplastic properties of thin layers on the substrate what gives expected effects. Selected, important, practical applications of coatings tribology are presented in figures 1 and 2 (Holmberg et al., 1998). It is seen in figure 1 that thin hard coatings on a soft substrate generate lower stresses in the coating and at the coating/substrate interface compared with thick hard coatings with the same deflection. Figure 2 shows the multilayer coating with alternate hard and soft layers allowing deflection to occur under load without yielding of the hard layers. They slide over each other, with shear occurring in the soft layer. The pattern of shear is illustrated by the line through the film, which was initially straight in the unloaded condition. These features and many others fundamentals of coatings tribology are used in designing of multilayer system.

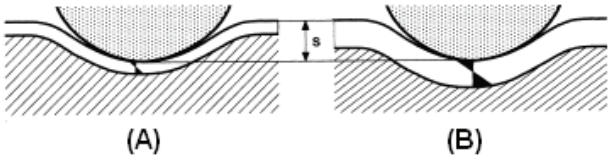

Figure 1. Stresses generated at the coating/substrate interface by thin (A) and thick (B) hard coatings on a soft substrate with the same deflection.

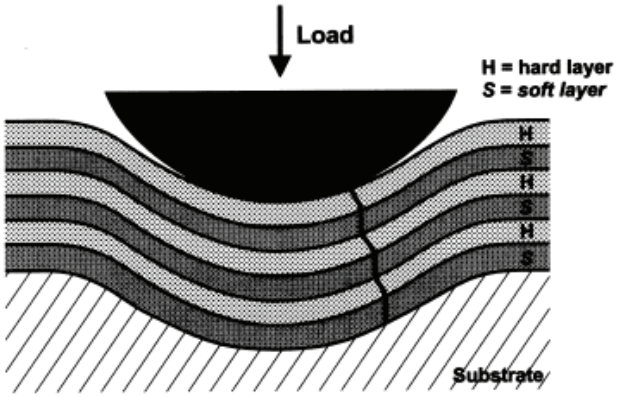

Figure 2. A multilayer coating with alternate hard and soft layers on a soft deflected substrate.

Hard coating systems are analyzed. They consist of titanium nitride basis and thin mixed elastoplastic multilayers, which are deposited on the elastic substrate. Two systems are considered, namely:

- system 1 – MT-CVD (medium temperature chemical vapour deposition), which is composed of three, thin material layers on carbide,
- system 2 – PVD (physical vapour deposition), which is composed of eleven, thin material layers.

Systems 1 and 2, which are technical materials, are presented in figures 3 and 4. Each coating shows material layer used in material system.

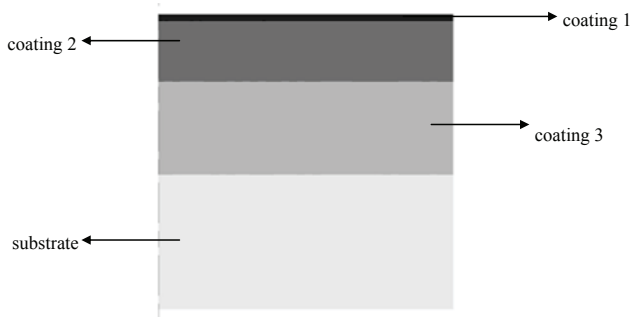

Figure 3. System 1 is shown as three different coatings depos

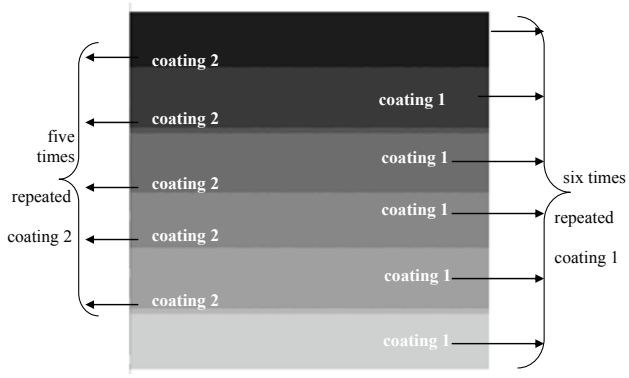

Figure 4. System 2 is shown as two different coatings deposited periodically, respectively coating 1 is repeated six times and coating 2 is repeated five times. Coating 2 is very thin.

Table 1. System 1. Elastic properties of layers used in system 1.

Material	coating 1 (Cai and Bangert, 1996)	coating 2 (www.matweb.com)	coating 3 (Santhanam et al., 1996; Fang et al., 2004)	substrate (FORGE® V.2.4 materials database)
Elastic modulus, GPa	616	370	535	683
Poisson ratio	0.25	0.22	0.25	0.3
width of layer, μm	22.0			

Table 2. System 2. Elastic properties of layers used in system 2.

Material	coating 1 (Zoestbergen, 2000)	coating 2 (Cai and Bangert, 1996)
Elastic modulus, GPa	380	616
Poisson's ratio	0.177	0.25
width of layer, μm	2.6	

2.2. Material properties

Elastic properties of each layer used in the model for system 1 are given in table 1. Coating 1 and coating 2 are characterized by both elastic and plastic properties, and that is why the elastoplastic bilinear material models ($\sigma_f = \sigma_0 + A\varepsilon$) are used for them. The parameters of the model are:

- Coating 1 (Cai and Bangert, 1996), yield strength σ_0 = 5000 MPa, strain hardening A = 50 GPa;
- Coating 2 (www.matweb.com), yield strength σ_0 = 3000 MPa.

Elastic properties of each layer used in simulations for system 2 are given in table 2.

Additionally, as in system 1: Coating 2 (Cai and Bangert, 1996), yield strength σ_0 = 5000 MPa, strain hardening A = 50 GPa.

The FEM model of the specimen is axisymmetric. Thickness of each layer is smaller than its width, but the details are not revealed by the manufacturer.

2.3. Material models in FEM model

FEM is commonly used in simulation of thermal, mechanical and microstructural phenomena in material processing, especially metal forming and typical metals and alloys manufacturing processes. In this paper these solutions are adapted to a new objective, which is specified as a prediction of nano-systems behaviour and state of strains under low load (Beake and Smith, 2004), which is here characterized by high strain rate indentation (indentation under high-strain rate loading). Prediction of small propagation, location and value of plastic deformation in the nano-systems is the objective of the simulations.

Thin films create new numerical problems. These difficulties arise from layers thickness, necessity of remeshing, multi-material and multi-impact character of simulation, which has to connect different types of numerical solutions simultaneously. Thus, direct jump from experiment to simulation cannot be made without some simplifications of the model and assumptions, which are pointed out and described in the paper.

The Forge 2 program (The Forge V.2.4, 2004) is designed for forging simulation in various conditions. This FEM based computing code solves numerical problems related to large deformations, which occur in mesh elements during process. Initial mesh is being rebuilt, when it is necessary (mesh elements are too deformed) and it is called remesh-

ing operation. Since considered case needs new mesh generation in many computing steps, the Forge 2 code is chosen. Some numerical problems arise and they are related to very small thickness of coating 2 in system 2. Due to remeshing procedure, more than one node (minimal number of nodes is three for good accuracy of calculations) must be generated on a very small distance (equal to thickness of coating 2). During remeshing procedure new elements are created and more nodes are required.

The description of the rheology of the material in Forge 2 is based on the Norton-Hoff flow rule written in the following form (Chenot and Bellet, 1992):

$$\boldsymbol{\sigma} = 2K(T,\bar{\varepsilon},...)\left(\sqrt{3}\dot{\bar{\varepsilon}}\right)^{m-1}\dot{\boldsymbol{\varepsilon}} \qquad (1)$$

This relation links the deviatoric stress tensor $\boldsymbol{\sigma}$ to the strain rate tensor $\dot{\boldsymbol{\varepsilon}}$ through the consistency $K(T,\bar{\varepsilon},\ldots)$ and the sensitivity to the strain rate m. The theoretical behaviour corresponding to the value m = 1 also called Newtonian behaviour, can also be integrated in Forge 2. In this case, the set of equations describing the problem of mechanical equilibrium is linear. In equation (1) T is absolute temperature, $\bar{\varepsilon}$ is effective strain and $\dot{\bar{\varepsilon}}$ is effective strain rate.

Elasto-viscoplastic flow rule is used, which is integrated as an elastoplastic law. The flow stress is related to strain hardening, strain rate and the temperature following the equation:

$$\sigma_f = \sqrt{3}^{(1+m)} K_0 (1+a\varepsilon)\exp\left(\frac{\beta}{T}\right)\dot{\varepsilon}^{m} \qquad (2)$$

According to material properties specified above on the basis of (Cai and Bangert, 1996; www.matweb.com), values given in table 3 are introduced into equation (2). The remaining material layers are elastic and only elastic properties given in Tables 1 and 2 are required in material models.

The dynamic implicit version of Forge2 code is used for both hot and for cold forging simulations. As it was mentioned the description of the material rheological behaviour is based on the elastoplastic law, which states that the following assumption for the material is true: at every moment it is possible to separate the instantaneous deformation in the elastic reversible part $\bar{\varepsilon}_e$ and plastic irreversible part $\bar{\varepsilon}_p$, as follows:

$$\bar{\varepsilon} = \bar{\varepsilon}_p + \bar{\varepsilon}_e \qquad (3)$$

Table 3. Values of material parameters used in FORGE 2 simulations

System / Coating	Equation parameters	a	β, K	K_0, MPa	m
System 1					
Coating 1		12.5	0	1154.7	0
Coating 2		16.949	0	1703.18	0
System 2					
Coating 2		12.5	0	1154.7	0

Elastic behaviour

Part of the material deformation is represented by a reversible elastic behaviour, which is idealized through the linear elasticity law (Hook law). For small strains this is written as:

$$\Delta\boldsymbol{\varepsilon} = \frac{1+\nu}{E}\boldsymbol{\sigma} + \frac{3\nu}{E}p\mathbf{I} \qquad (4)$$

where $\mathbf{I}$ - unit tensor, $\Delta\boldsymbol{\varepsilon}$ - the elastic small strains tensor, $\boldsymbol{\sigma}$ - the stress tensor. The material parameters are Young modulus E and the Poisson ratio v. These parameters are supposed to be constant and are entered in the data file. Their values for the investigated materials are given in tables 2 and 3.

Hydrostatic pressure is given by the formula:

$$p = -\frac{1}{3}trace(\boldsymbol{\sigma}) \qquad (5)$$

Plastic behaviour

When the material behaviour is considered as elastoplastic, the description of the variables related to the plastic part of the deformation is based on the Huber-von Mises criterion. A simplified way of describing this criterion is:

if $\sigma_{eq} = \sigma_f$: plastic deformation occurs

if $\sigma_{eq} < \sigma_f$: elastic deformation occurs

where σ_{eq} is the effective stress and is defined as one of the stress tensor invariants with the following expression:

$$\sigma_{eq}^2 = \tfrac{1}{2}[\,(\sigma_{xx}-\sigma_{yy})^2 + (\sigma_{yy}-\sigma_{zz})^2 + (\sigma_{zz}-\sigma_{xx})^2\,] \qquad (6)$$

and σ_f is called the yield stress (limit of the plastic strain domain).

3. LABORATORY TEST

Detailed information about the impact test, such as settings and conditions set in numerical model, as well as data used for validation the model, are taken from Beake at al. (2004). The pendulum impulse

impact option of the Nano Test System (Micro Materials) is applied for the nano-impact testing in this test. A solenoid connected was used to produce the probe impacts on the surface, as shown schematically in figure 5. A blunt (tip radius; 150nm) Berkovich diamond indenter test probe is accelerated from a distance of 12μm from the surface to produce each impact with a maximum impact force. Description of the Berkovich probe can be found in ISO 14577-2:2002 and ISO 14577-1:2002. The experiments were computer controlled so that repetitive impacts occur (at the same position) every 4s. Twenty repeated tests, each of 300s duration, were performed at different locations on each sample.

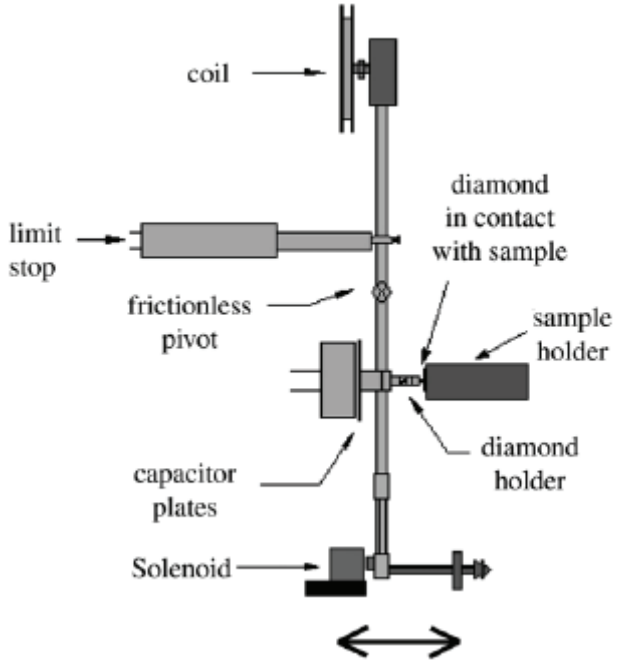

Figure 5. Schematic illustration of the Nano Test System showing the configuration for impact testing (Beake et al., 2004).

4. NUMERICAL TEST

Forge 2 (FEM program) uses dynamic implicit version of FEM. Numerical nano-impact test conditions are supposed to reproduce those in laboratory test, but there are some simplifications introduced. Berkovich rigid probe with sharp tip (tip radius 150nm) was accelerated from a distance s of 12μm from the surface to produce each impact with minimum impact force F of 100mN. This moving tool was set as a hummer press in program. Initial conditions of this press are: velocity v, mass of falling m, kinetic energy E_K and height h. Knowing force and die displacement, mass and velocity are calculated and set into the program. These loading variables are obtained from following relations:

– for mass:

$$W = E_P = mgh$$
$$W = Fs = mgh \Rightarrow m = \frac{Fs}{gh} \tag{7}$$

– for velocity:

$$E_P = E_K = \frac{mv^2}{2}$$
$$mgh = \frac{mv^2}{2} \Rightarrow v = \sqrt{2gh} \tag{8}$$

In relation (7) work W is equal to potential energy E_P and mass m is calculated. In relation (8) potential energy E_P is equal to kinetic energy E_K and velocity v is obtained.

Applying 2D and axisymmetric numerical model is justified here and it does not cause loosing important information. Due to high computing costs, number of impacts is fixed to 20 which differs from laboratory test. In experimental indentation test loading is set in 20 steps and high rate indentation is made. The number of deformation steps in numerical impact test is equal to number of deformation steps in indentation experimental test with Berkovich indenter. The idea of above numerical test (high strain rate indentation suggestion) was given by authors of (Beake and Smith, 2004). Additionally, but there is no need to set more impacts, because there is no fatigue and crack criterion in the present FEM model. Naturally, cracks are detected in the laboratory test. In this paper plastic deformation is shown, not fracture mechanism with cracks or debris. Actually, simulation cannot predict crack effect, but it is Authors plan of further research to improve the FEM model by implementing crack criterion.

Coulomb friction law is used in simulations. Friction coefficient μ in die-specimen contact region (nodal contact) is equal to 0.12. In experiment friction is an unwanted parameter, but there is no possibility to get such ideal conditions in deformation process.

Numerical model is an initial FEM model of thin, hard coating systems in impact test. In this paper simulation of impact test shows deformation pattern and cannot be quantitatively compared to experimental test. It allows qualitative validation only. Simulation is rather based on experiment (precisely on two experiments: nano-impact test and nanoindentation test) and can be called simulation of high strain rate indentation (high strain rate deformation process) in present work.

4.1. Hard coating system 1

4.1.1. Numerical model and results

The following numerical model for the hard coating system 1 is set: number of nodes 5854, number of triangular elements 11258. Multilayer specimen discretization for FEM analysis is presented in figure 6. Initial, numerical, axisymmetric model is used to model the test. The initial mesh is presented in figure 6A. Four material layers can be distinguished, as well as Berkovich rigid die with sharp tip and lower fixed die. Enlargement of the zone of interest, which is die-specimen contact region, is shown in figure 6B. Local mesh refinement in the program leads to fine mesh in the contact region. Application of remeshing allows simulating highest stroke of the tool and improves accuracy of simulation.

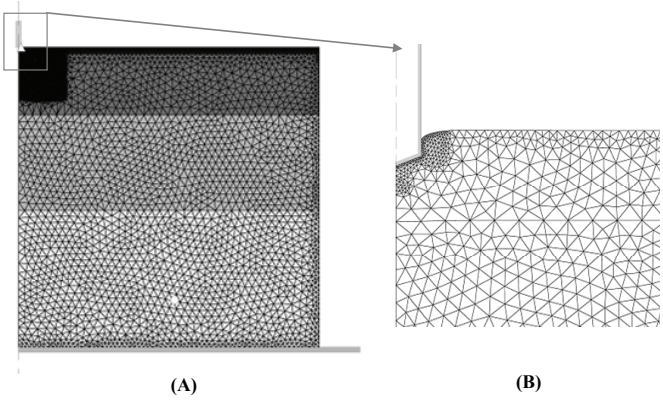

Figure 6. (A) Specimen and dies before deformation; (B) Weakly deformed contact region between specimen and moving die.

Due to its meaning in the model, specimen-die contact region is chosen as a zone of interest. In this zone deformation initiates and spreads out. Distributions of effective strain and pressure in this zone are presented in figure 7. Effective stress is defined by equation (6) and effective strain (equivalent strain) ε_{eq} by:

$$\varepsilon_{eq} = \int_0^t \sqrt{\frac{2}{3}\dot{\boldsymbol{\varepsilon}}_{ij}\dot{\boldsymbol{\varepsilon}}_{ij}}\,dt \tag{9}$$

where: $\dot{\boldsymbol{\varepsilon}}_{ij}$ – strain rate tensor.

The most irreversibly deformed parts are coating 1 and coating 2. They have the highest value of strain, what is visible in strain zone in figure 7. Looking at these plots it is obvious that sharp tips of Berkovich rigid die form sources of plastic deformation waves, which are shown as distributions of effective stress in the specimen. Some die surface irregularities occur in the strain distribution at the end of the test.

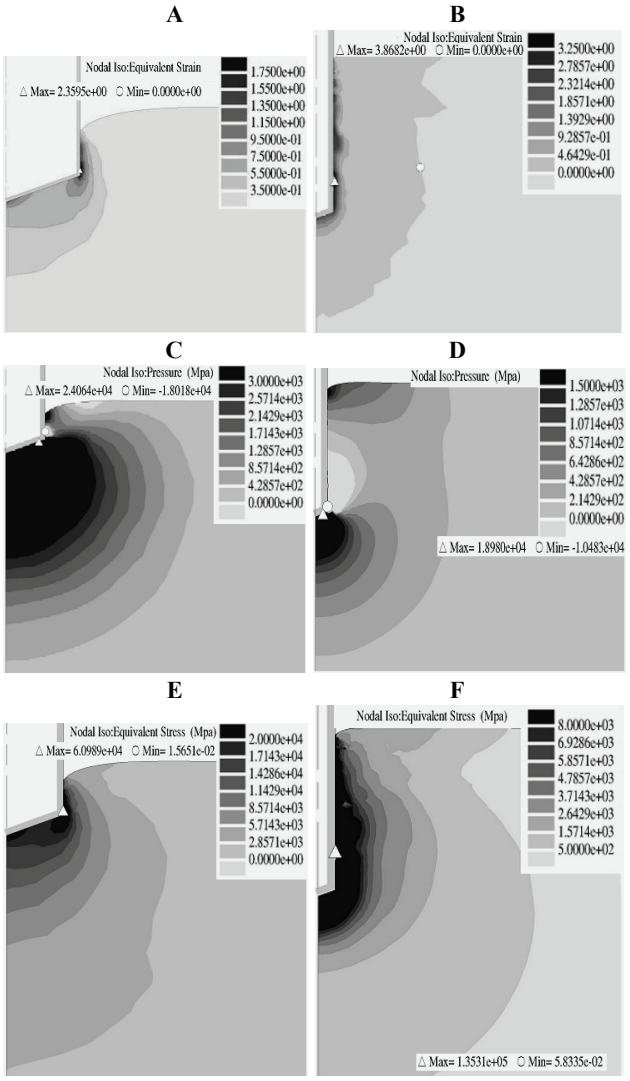

Figure 7. Calculated distributions of effective strain (top: A, B), pressure (centre: C, D) and effective stress (bottom: E, F). Beginning of the impact test (left A, C, E); end of the impact test (right B, D, F).

Effective stress and pressure distributions have comparable values in the whole test and reach maximally tens of GPa. The maximum values are received in die/specimen contact region. Model predictive capability can be confirmed by time versus depth graph (figure 8A), which shows regularity and repeatability in penetration of a specimen during tests and proves that it happens gradually. Figure 8B presents results with a continuation of the time scale and gives additional explanation that each impact does not run along straight line, like in elastic materials. In spite of elastic character of bottom layers, material behaves as not elastic medium, what is due to plastic character of thin coating 1 and coating 2.
Remeshing procedure also has a visible effect on total time increment versus depth curves, because they are not smooth and have rather jagged character. In experiment jagged shape of time versus depth curve is caused by fracture, because cracks occur

during high strain rate deformation process. The shape of time versus depth graph agrees quantitatively with the experimental one showed by (Beake and Smith, 2004). Number of time increments is not constant in each impact, it changes during computing process and depends on mesh deformation in contact region (number of remeshing procedures).

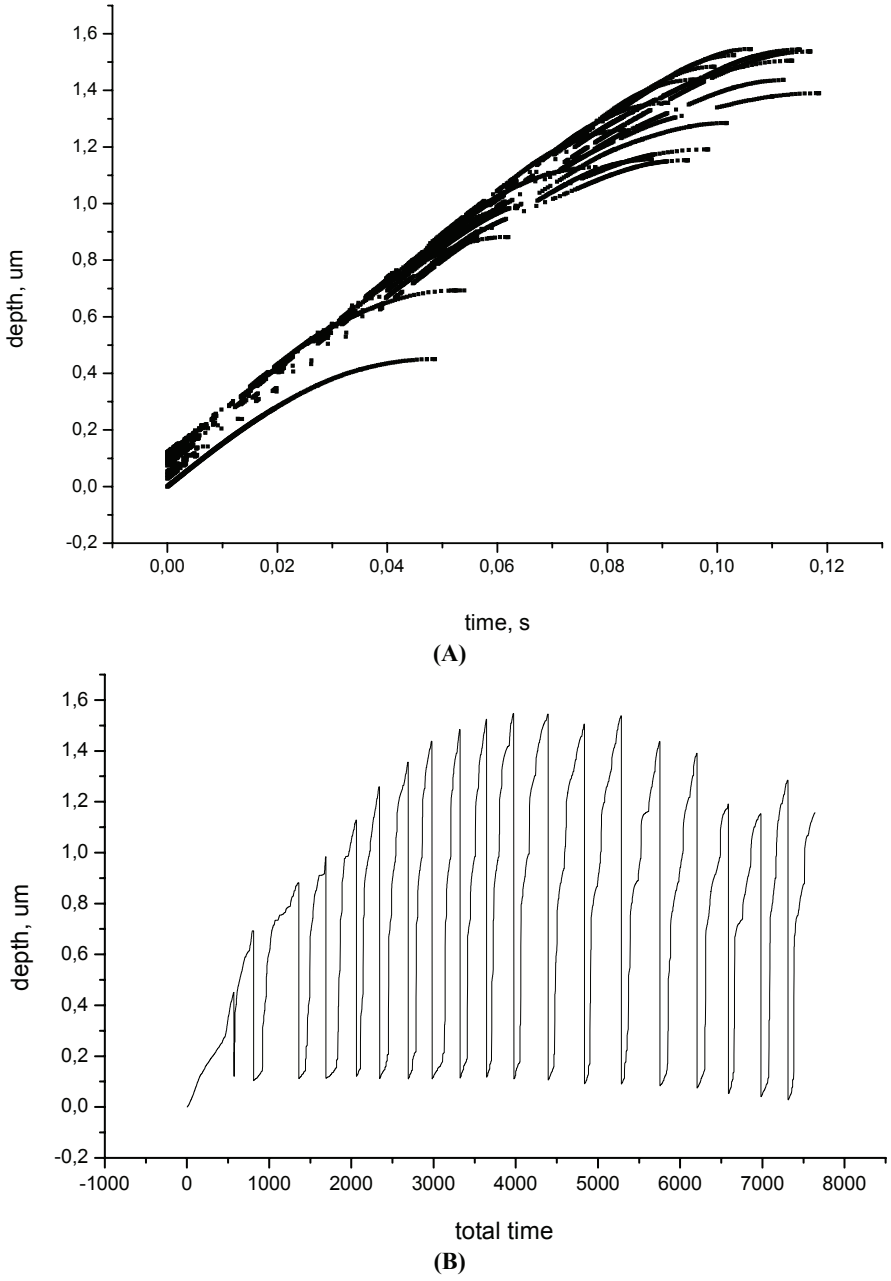

Figure 8. Numerical predictions of depth versus time starting from zero point for each stroke (A), Depth versus total time (B).

Having information about correctness of computational model, further results can be considered like pressure distribution in the whole specimen as in figure 9, which shows plastic deformation zones. The most interesting is surface-character of pressure wave, which occurs also at the bottom of specimen, but it is rather caused by specimen shape, boundary conditions and 2D model (2D is interpreted as cross-section of the specimen). Different shapes of samples and die and other boundary conditions are not examined in present paper.

Further application of the numerical model to the inverse analysis requires sensitivity analysis. It has already been performed by authors (Kopernik and Szeliga, 2007). Observed bottom pressure waves cannot be completely left out of account, but their influence on the model is small and caused by elastic character of bottom material layers, which do not cumulate deformation as plastic layers do. Plastic deformation appears in maximum pressure zones, what is related to material properties – top layers are elastoplastic medium. These distributions are calculated after unloading, when they present residual pressure zones in material, and before unloading, when they present pressure zones under loading. In figure 9 are presented selected results for impact number 1, 5, 10, 15 and 20.

Graph showing plastic power versus depth of indentation (figure10) is used to locate the maximum plastic response of the hard coating system 1 (depth is not treated as a time scale). Plastic power it is an integral over the all finite elements of mesh where plastic strain occurs. The maximum value of plastic power occurs, when the maximum depth penetration is equal to 0.9 μm (the highest depth was chosen at the end of deformation process). Comparing occurrence of the maximum plastic power with figure 8b (showing depth versus time increment), it is obvious that the depth penetration is equal to 0.9 μm in the third impact, before quarter of the test. Additionally, according to the geometry of the system 1, when the penetration depth reaches 0.9 μm, this value of the penetration depth corresponds to the thickness level of coating 2.

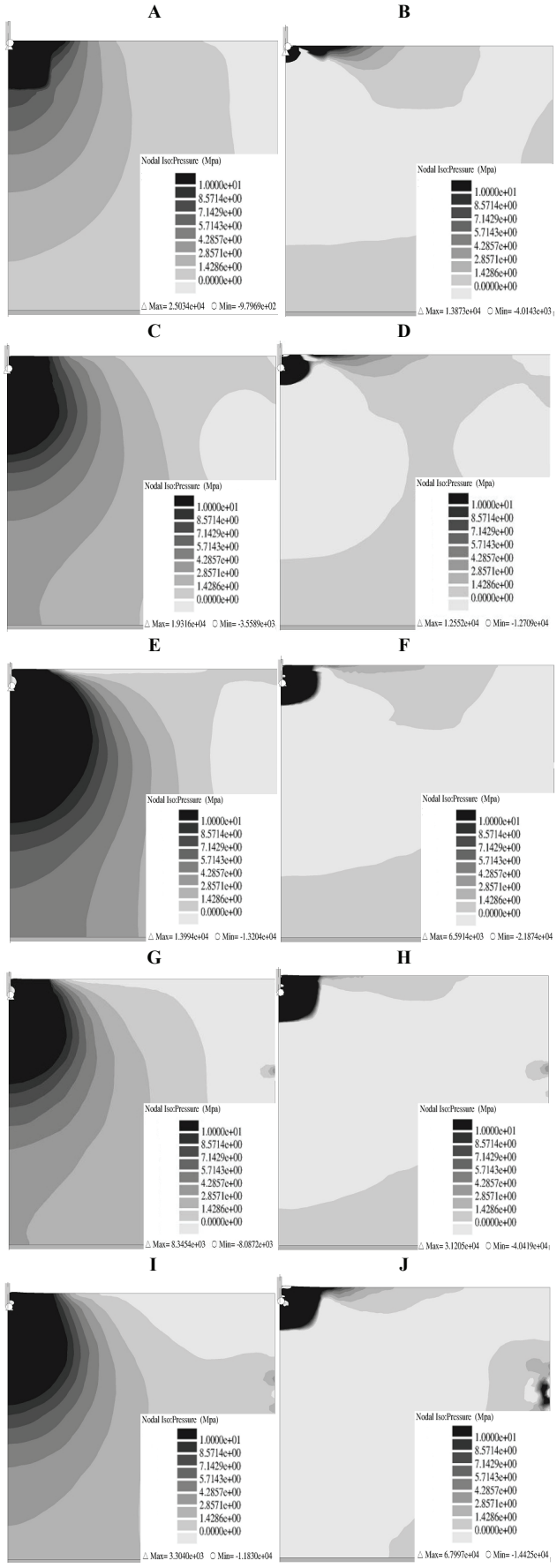

Figure 9. Plots showing distributions of pressure computed every five impacts, before unloading/first blow (left A, C, E, G, I) and after unloading/final blow (right B, D, F, H, J).

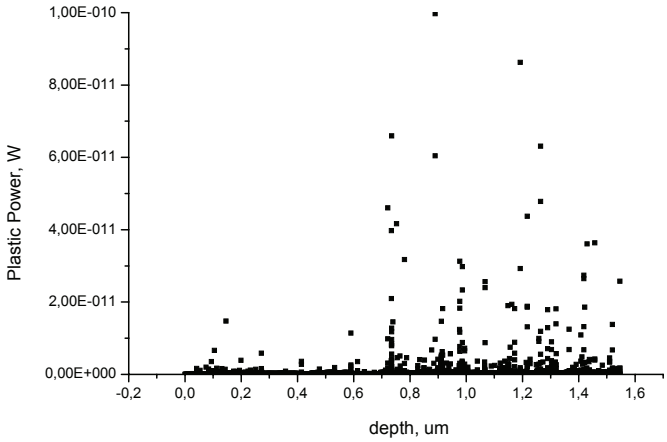

Figure 10. Plastic power versus depth of indentation.

4.2. Hard coating system 2

4.2.1. Numerical model and results

The numerical model for the hard coating system 2 is composed of 3395 nodes and 6608 triangular elements. Multilayer specimen FEM discretization is presented in figure 11. Axisymmetric, numerical model is used in the simulation and it is shown as the initial mesh in figure11A. Eleven material layers can be distinguished, as well as the Berkovich rigid die with sharp tip and the lower fixed die. Enlargement of the zone of interest, which is die-specimen contact region, is shown in figure 11B. Local mesh refinement in the program leads to fine mesh in contact region. Remeshing is introduced similarly as for the coating system 1, enabling analysis of larger die strokes and improving accuracy of the model.

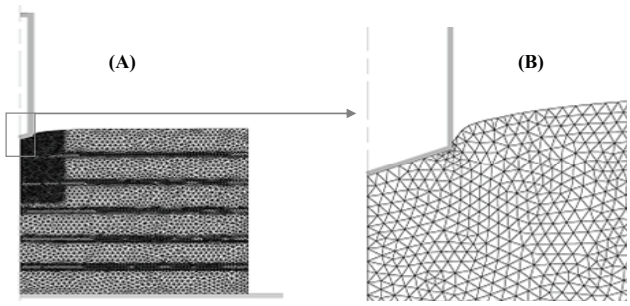

Figure 11. (A) Specimen and dies during deformation; (B) Weakly deformed contact region between specimen and moving die.

Due to its meaning in the model, specimen-die contact region is chosen as the zone of interest. In this zone deformation initiates and spreads out. Because of elastic character of the first deformed layer, irreversible deformation occurs in plastic zones in Coating 2, where the highest plastic strain occurs. It is visible in strain zone in figure 12. Looking at this plot it is obvious that sharp Berkovich shape rigid tip

forms sources of plastic deformation waves, which are shown as distributions of pressure and effective stress in the specimen. In sandwich elastoplastic coupled hard coating system 2 the coating 2 cumulates deformations, while the elastic coating 1 transmits loadings and acts during unloading.

Hard coating system 2 is a sandwich multilayer system with coupled elastoplastic character and proceeding analysis is carried out similarly as for the hard coating system 1. Distributions of computed values are regular and concentrated in the centre of the specimen.

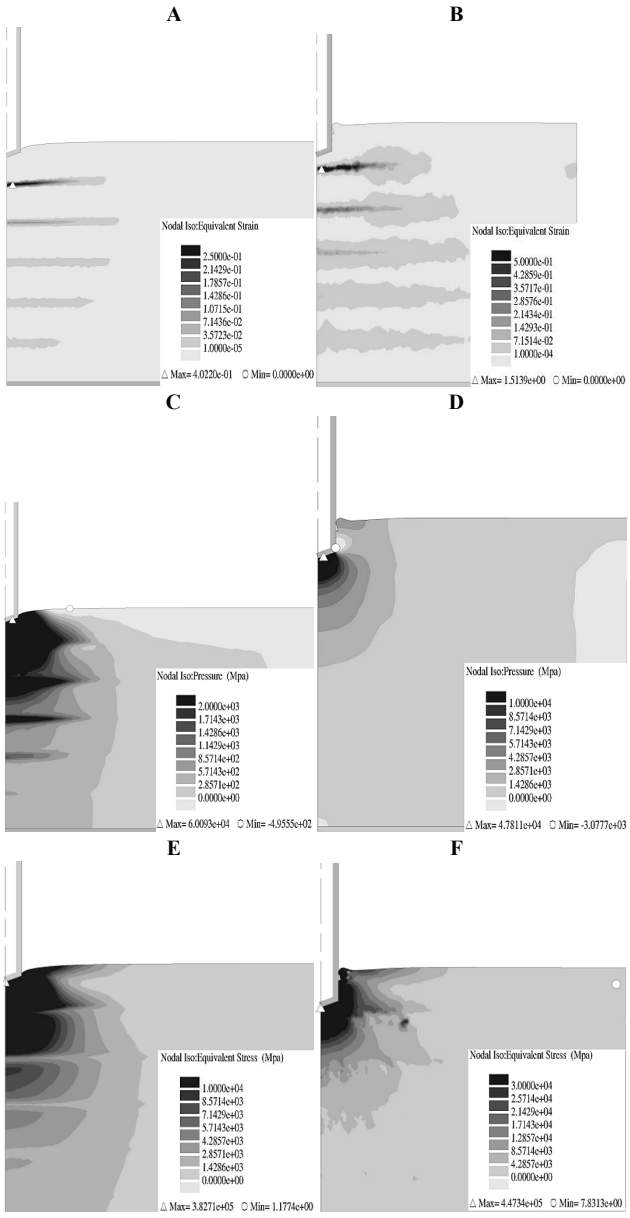

Figure 12. Calculated distributions of effective strains (top: A, B), pressure (centre: C, D) and effective stresses (bottom: E, F). Beginning of the impact test/first blow (left A, C, E, G); end of the impact test/final blow (right B, D, F, H).

Time versus depth graph is presented in figure 13A, which shows regularity and repeatability in penetration of a specimen during each impact and proves that it happens instantaneously. These results confirm good predictive capability of the model. Figure13B presents results with a continuation of the time scale and gives additional explanation that the maximum value is reached and remains at this level. This graph also proves that each impact does not run along straight line, like in elastic materials. In spite of elastic character of coating 1, material behaves as not elastic medium, what is due to plastic character of thin coating 2.

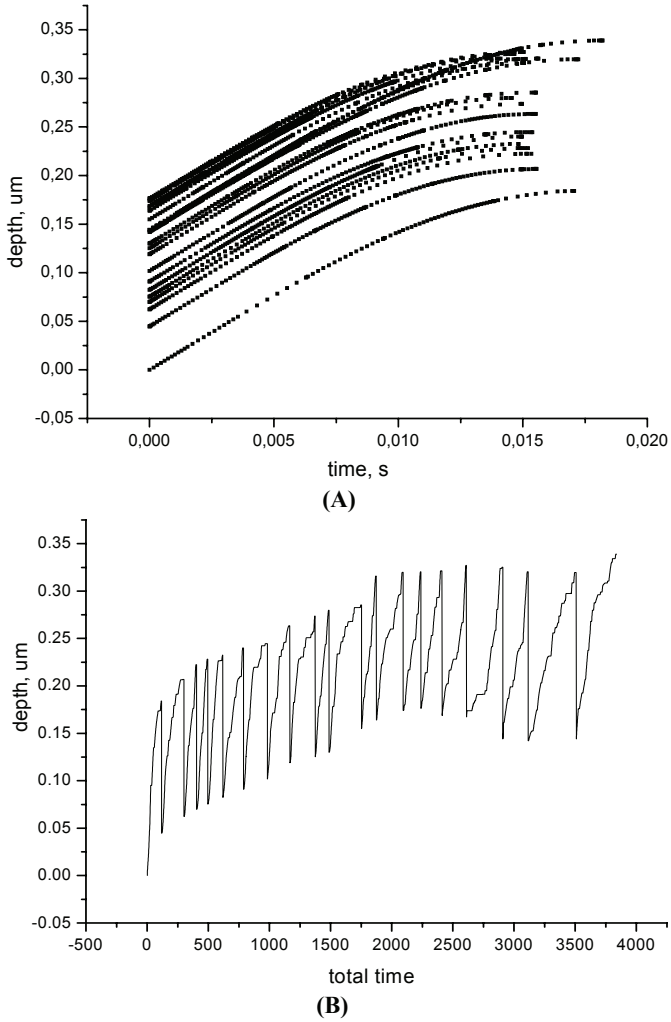

Figure 13. Depth versus time starting from zero point for each stroke (A), Depth versus total time (B).

Monitoring of calculated pressure (Figure 14) shows that plastic deformation appears in maximum pressure zones, what is related to material properties: coating 1 is elastic and coating 2 is elastoplastic medium. Distributions calculated after unloading present residual pressure zones, which are concentrated in zones of elastoplastic material, and they are smaller than those calculated before unloading. Distributions computed before unloading present pressure zones under loading and are almost uniformly spread in the whole specimen.

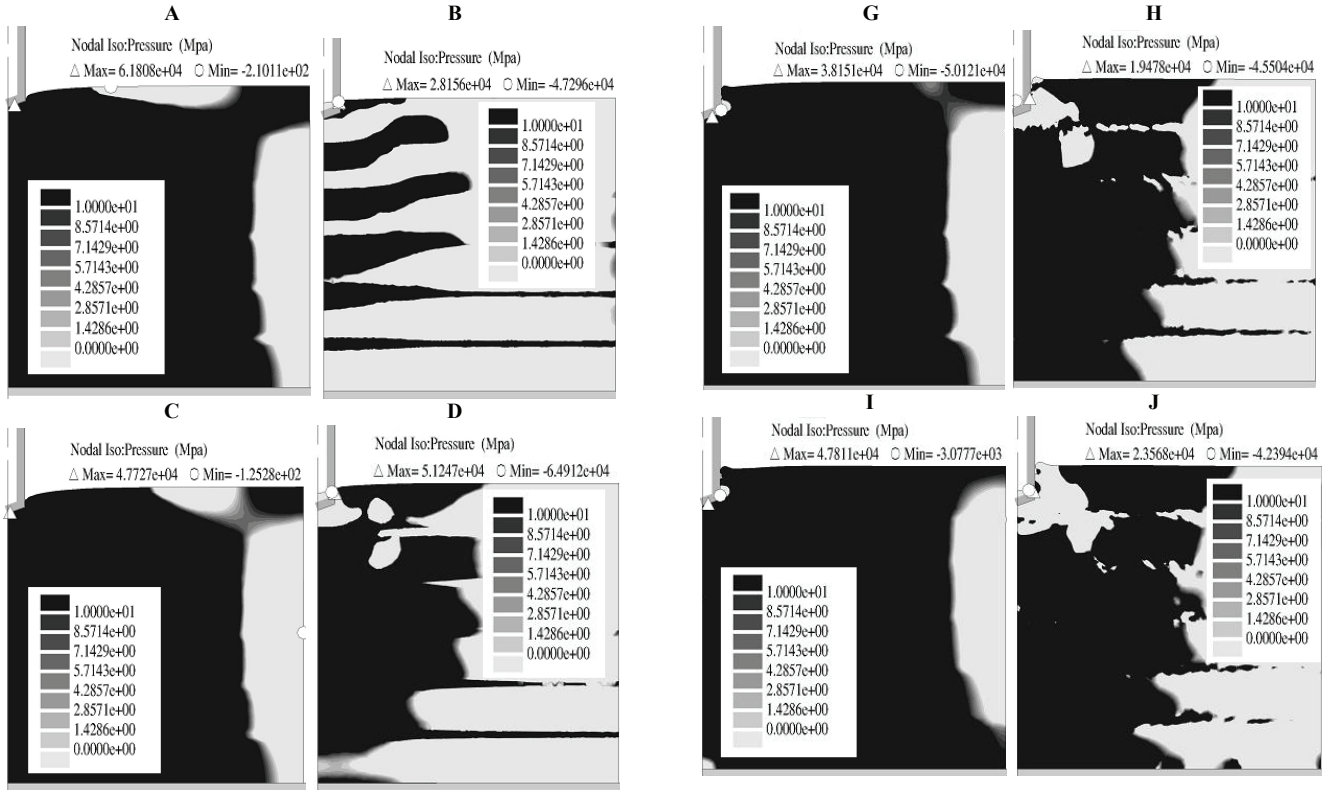

Figure 14. Monitoring of calculated distributions – distributions of pressure computed every five impacts. End of the impact no. 1 (A,B), 5 (C,D), 10 (E,F), 15 (G,H) and 20 (I,J). Before unloading/first blow (left A, C, E, G, I) and after unloading/final blow (right B, D, F, H, J).

Graph showing plastic power versus depth (figure15) can be used to locate the maximum plastic response of the hard coating system 2. The maximum value of plastic power occurs, when the maximum depth penetration is equal to 0.25μm. Comparing occurrence of the maximum plastic power with figure 13B, which shows graph depth versus time increment, it is obvious that the depth of penetration is equal to 0.25 μm in the 8-th impact, before half of the test. Beyond this, according to geometry of the system 2, when the penetration depth reaches 0.25 μm, this value of the penetration depth corresponds to the thickness level of the coating 1.

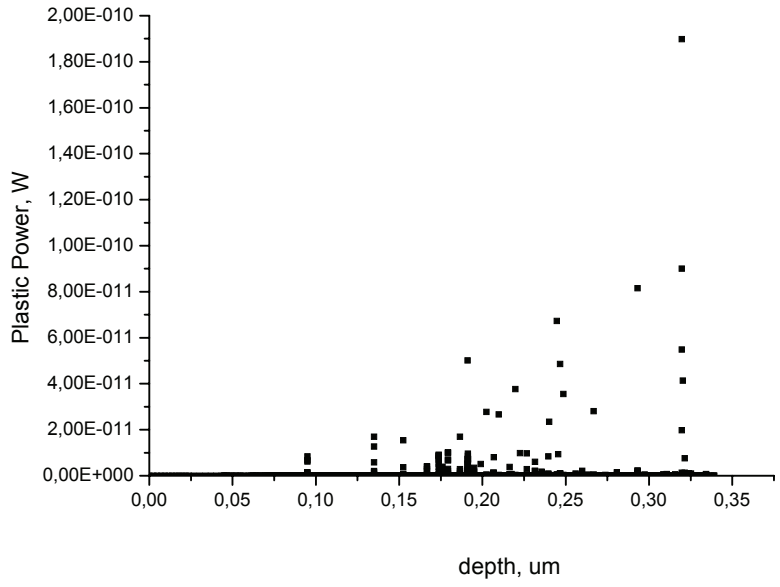

Figure 15. Plastic power versus depth of indentation.

5. CONCLUSIONS

Numerical simulations were performed for the nano-impact tests for the two systems. The predictive capability of the FEM model has been confirmed and possibility of its application to the interpretations of the tests was proved. Several conclusions can be drawn from the results of simulations and they are sum-

marized below.

The same initial impact test conditions for both cases allowed comparison of the two systems. In the hard coating system 2 stresses are one order of magnitude greater than in the hard coating system 1. In the second system distributions are inside specimen and in the first system they have surface character. The maximum plastic power in the hard coating system 2 has multiple value of maximum plastic power in the hard coating system 1. In the hard coating system 2 there is a greater contribution of plastic zones than in hard coating system 1.

Acknowledgements: Financial assistance of the MNiSzW, project no. 11.11.110.643, is acknowledged.

REFERENCES

Beake, B.D., Lau , S.P., Smith, J.F., 2004, Evaluating the fracture properties and fatigue wear of tetrahedral amorphous carbon films on silicon by nano-impact testing, *Surface and Coatings Technology*, 177 –178, 611–615.

Beake, B.D., Smith, J.F., 2004, Nano-impact testing - an effective tool for assessing the resistance of advanced wear-resistant coatings to fatigue failure and delamination, *Surface and Coatings Technology*, 188–189, 594–598.

Cai, X., Bangert, H., 1996, Finite-element analysis of the interface influence on hardness measurements of thin films, *Surface Coatings Technology*, 81, 240-255.

Chenot, J.L., Bellet, M., 1992, The Viscoplastic Approach for the Finite-Element Modelling of Metal Forming Processes, In,: *Numerical Modelling of Material Deformation Processes*, eds, Hartley, P., Pillinger, I., Sturges, C.E.N., Springer-Verlag, London, Berlin, 179-224.

Dao, M., Gu, P., Maewal, A., Asaro, R.J., 1997, A micromechanical study of residual stresses in functionally graded materials, *Acta Mater.*, 45, 3265-3276.

Fang, T.-H., Jian, S.-R., Chuu, D.-S., 2004, Nanomechanical properties of TiC, TiN and TiCN thin films using scanning probe microscopy and nanoindentation, *Applied Surface Science*, 228, 365–372.

The FORGE® V.2.4 materials database, 2004, Transvalor SA, Sophia-Antipolis, France.

Hansel, A., Spittel, T., 1978, *Krafts und Arbeitsbedarf Bildsamer Formgebungverfahren VEB Deutscher Verlay fűr Grundstoff Industrie*, Leipzig.

Holmberg, K., Matthews, A., Ronkainen, H., 1998, Contact mechanism and surface design, *Tribology International*, 31, 1–3, 107–120.

http://www.matweb.com/search/SpecificMaterial.asp?bassnum=BA1A

Kopernik, M., Pietrzyk, M., 2006, Evaluation of possibilities and perspectives of application of nanomaterial hard coatings, *Computer Methods in Materials Science*, 6, 42-63.

Kopernik, M., Szeliga, D., 2007, Modelling of nanomaterials – inverse and sensitivity analysis to determine material parameters, *Computer Methods in Materials Science,* 7, 255-261.

Kopernik, M., Pietrzyk, M., 2D numerical simulation of elasto–plastic deformation of thin hard coating systems in deep nanoindentation test with sharp indenter, *Arch. Metall. Mater.*, 2007, (in press).

Paszyński, M., Kopernik, M., Madej, Ł., Pietrzyk, M., 2006, Automatic hp adaptivity to improve accuracy of modeling of heat transport and linear elasticity problems, *J. Machine Eng*., 6, 73-82.

Santhanam, A.T., Quinto, D.T., Grab, G. P., 1996, Comparison of the steel-miling performance of carbide inserts with the MTCVD and PVD TiCN coatings, *Int. J. of Refractory Metal and Hard Materials*, 14, 31-40.

Zoestbergen, E., 2000, X-ray analysis of protective coatings, http://dissertations.ub.rug.nl/FILES/faculties/science/2000/e.zoesterbergen/c5.pdf.

Zienkiewicz, O.C., Taylor, R.L., 2000, *The Finite Element Method*, Butterworth-Heinemann, Oxford.

NUMERYCZNA SYMULACJA ODKSZTAŁCENIA SPRĘŻYSTOPLASTYCZNEGO UKŁADÓW CIENKICH, TWARDYCH POWŁOK W TEŚCIE UDARNOŚCI

Streszczenie

Celem pracy jest rozwój modelu na bazie metody elementów skończonych (MES) do symulacji testów udarności dla układów twardych nanopowłok. Wymienione testy są wykonywane, aby określić odporność materiału na pękanie. Do przedstawionego w pracy modelu MES nie wprowadzono kryteriów pękania. Pokazano jedynie jak zachowuje się materiał pod wpływem obciążenia udarowego. Trudności prowadzenia symulacji wynikają z małej grubości powłok, konieczności wykonania aktualizacji siatki elementów (remeshingu), wielomateriałowego i wieloetapowego charakteru modelu MES, który musi połączyć różne rodzaje rozwiązań numerycznych jednocześnie. Symulacje wykonano za pomocą kodu FORGE 2, który przystosowano do warunków i wymagań istniejących w układach powłok i w modelowanym matematycznie doświadczeniu. W publikacji zamieszczono wyniki symulacji dla testów udarności opracowanych dla dwóch układów nanopowłok. Wykazano, że stworzony model potrafi przewidywać rozkłady intensywności naprężeń i odkształceń oraz można do niego wprowadzić kryteria pękania, które korzystają z obliczanych w modelu wartości naprężeń i odkształceń.

Submitted: May 8, 2006
Submitted in a revised form: September 26, 2006
Accepted: January 3, 2007